Corrosion of Steel Pipes Utilized for Crude Oil Production and Transportation in Oil and Gas Industry

Sayed Dobl[1*], A. A. Omar[2], M. Gouda[2], Salah Salman[2, 3], Ibrahim M. Ghayad[4]

[1]Petroleum and Mining Engineer, Agiba Petroleum Company, Cairo, Egypt

[2]Mining & Metallurgy Eng. Dept. Faculty of Engineering, Al-Azhar University, Cairo, Egypt

[3]Institute of Innovation for Future Society, Nagoya University, Nagoya, Japan

[4]Corrosion Control and Surface Protection, Central Metallurgical Research and Development Institute | CMRDI, Cairo, Egypt

*Corresponding author: E-mail: Eng.sss85@hotmail.com (Sayed Dobl)

Abstract

The corrosion behaviour of two carbon steel alloys used in the production and transportation of oil was investigated in CO_2 saturated solution, as a function of chloride ions content, at ambient temperature and pressure. The study used electrochemical measurements, including potentiodynamic polarization and electrochemical impedance spectroscopy (EIS). Both alloys showed a peak value at 3.5 wt. % NaCl, followed by a drop on further chloride ion increases up to 15 wt. % NaCl. Nevertheless, the second alloy (2) showed a much better performance and lower corrosion rate, which could be related to composition, grain size, and mechanical properties. Reduction in corrosion rates in spite of further addition of chloride ions was explained on the basis of reduction of CO_2 solubility or salting out and the role of chloride ions in accelerating iron dissolution, which are available then adsorbed through the electrolyte to the cathodic sites, reducing active sites on the substrate for further reduction of carbonic acid and bicarbonate.

1. Introduction

In the production and transportation of oil and gas, carbon steel is the most common construction material for tubing and piping. It is liable to corrosion degradation and loss of integrity due to the corrosive species contained in the flowing fluids. [1-2]. CO_2 is the chief corrosive agent in the production stream, accompanied by the formation of water from reservoirs, containing Cl^- ions, with a varying concentration, which reduces the passivation tendency of steel surfaces [3,4] leading to localized corrosion and degradation of steel pipeline integrity; meanwhile, CO_2 corrosion represents the major cause of pipelines failure resulting in a considerable economic impact. A number of relevant studies were carried out in order to understand the corrosion mechanism of mild steel in the presence of Cl^- ions containing saturated CO_2 solution and the role of containing Cl^- ions concentration on

CO_2 corrosion. For example, Hausler et al. claimed that, in saturated CO_2 media, Cl^- ions had a trivial contribution to the corrosion of mild steel [5]. Bian et al. reported that CO_2 gas could promote the release of ferrous ions from steel surface to aggravate its corrosion degree in Cl^- containing solution (0.1 mol/L) [6]. However, Liu and colleagues investigated the corrosion mechanism of mild steel at a condition of 20 bar CO_2 partial pressure and 100 °C. Their results revealed that 25 g/ L Cl^- content in saturated CO_2 solution gave rise to a peak corrosion rate, while excess containing Cl^- ions played an inhibitory role in steel corrosion [7]. Meanwhile, Eliyan et al. studied the effects of Cl^- ions concentrations in 1bar CO_2 saturated solutions at 20 °C on corrosion of API-X100 steel, and proposed that a peak CO_2 induced corrosion rate of 185 $\mu A/cm^2$ was attained at 15 g/L NaCl

solutions [8]. Mao et al. found that the presence of small content of Cl could significantly reduce the passivation tendency of steel [9]. Chen found that localized corrosion became less obvious as Cl⁻content increased [10]. Sun et al. showed that Cl⁻content was important in the onset of localized corrosion because it has largely affected the ionic strength [11,12]. Ma et al. determined that the influence of Cl− content could lead to pitting [13]. In another study, Fang et al. demonstrated that CO_2 corrosion rate of carbon steel sharply decreased with increased salt concentration [14].

Jiang and Nesic also found that Cl⁻ content in concentrations between 1 and 20 wt% had no significant effect on localized corrosion rate at 80 ℃. Qu identified that NaCl improved the conductivity of CO_2 – saturated solutions, resulting in a quick dissolution of protective film on the surface of AZ31B [15]. Ingham et al. claimed that FeCO3 is the only phase formed in the NaCl solution in CO_2 corrosion at 80 ℃ [16]. However, Schmitt and colleagues identified that the susceptibility to pitting corrosion of pipelines attains a peak at 60–80 °C in a medium containing CO_2 [17,18]. It is apparent that the critical concentration of Cl⁻ ions in saturated CO_2 solutions that initiates the highest corrosion rate varies with testing circumstances.

It should be highlighted that the majority of investigations in the open literature have been done at high temperatures environments. In contrast, the crude oil that is being transported through pipelines flows at a temperature around room temperature. Although it is crucial to understand the mechanistic function that Cl⁻ ions play in CO_2 – saturated solutions when predicting the corrosion of transportation pipelines, research in this area is relatively lacking. The intends to explore the role of Cl⁻ ions on the corrosion behaviour of carbon steel in CO_2 – saturated solutions at room temperature, in order to address this information gap should be highly considered.

This study aims at investigating the effect of different Cl⁻ contents on CO_2 corrosion of two carbon steel alloys used in tubing and piping of oil production and transportation, in order to provide a comprehensive study of the mechanistic role of Cl⁻ content on the corrosion behaviour of carbon steel in CO_2 – saturated environment at ambient temperature and pressure.

2. Experimental

2.1. Materials

Two types of carbon steel alloys were selected to perform the study. which serve for crude oil production and transportation. Chemical analysis mechanical testing and microstructure were performed on these pipes material to identify their designations. The test specimens were cut from the steel pipes. The specimens were machined in order to perform electrochemical corrosion tests. Specimens were grounded progressively by sandpaper, washed with distilled water and dried immediately prior each test. One side of the test specimen was exposed to the saline solution, with an exposed surface area of 0.785 cm².

2.2 Methods

Electrochemical measurements were performed in different concentration of NaCl solution (1.5 - 15 wt %). Prepared by dissolving reagent grade NaCl in double distilled water, NaCl was chosen because it is the most common dissolved salt in the produced water accompanied hydrocarbon reservoirs. Another set of experiments were performed in NaCl solution saturated with CO_2 which was purged until a steady pH was reached.

Electrochemical measurements were carried out in a three-electrode corrosion cell with the tested sample as the working electrode, the reference electrode was saturated calomel electrode (SCE) and a platinum sheet working as a counter electrode. METROHM AUTO-LAB (PGSTAT302N) POTENTIOSTAT was used to perform polarization measurements.

The electrochemical corrosion tests performed for samples in four concentrations of sodium chloride namely; 1.5, 3.5, 10 and 15 Wt. % NaCl.

Electrochemical measurements were performed in CO_2 environment at 25 ± 2 °C. Sodium chloride (NaCl) powder was dissolved in deionized water to yield chloride ions containing solutions with varying concentrations (1.5, 3.5, 10 and 15 wt % NaCl). Solutions were then purged with CO_2 until a stable pH value of the solution was attained in order to yield saturated CO_2 solutions with various containing Cl⁻ ions concentrations. Additionally, the CO_2 gas purging was maintained throughout the test to ensure saturation.

Potentiodynamic polarization curves were scanned from - 0.3 to 1.0 V versus open circuit potential (OCP) at a scan rate of 5 mV/s. The obtained polarization curves were analyzed and fitted using the software Nova 2.1. Electrochemical impedance spectroscopy (EIS) measurements were conducted from 105 to 10−2 Hz.

3. Results

3.1. Material Characterization

The results of chemical analysis and mechanical properties tests of the investigated alloys showed that alloy1 is complying with API 5L Grade-B, while alloy2 is in conformity with API 5CT Grade L-80/1, the microstructure showed a ferritic – pearlitic structure of both alloys, meanwhile alloy2 has more fine grains.

3.1.1 Chemical composition

3.1.1.1 API 5L Standard 'Specification 5L covers steel line pipe' - Chemical Composition

Table-3.1: Chemical Composition – Mass fraction %.

Grade	C	Mn	P	S	V	Nb	Ti	Fe
	Max	Max	Max	Max	Max			Bal.
B	0.28	1.2	0.030	0.030	Sum < 0.15 %			
Alloy1	0.25	0.55	0.008	0.0005	0.003	0.004	0.004	98.2

3.1.1.2 API 5CT Standard 'Specification 5CT for Casing and Tubing' - Chemical Composition

Table-3.2: Chemical Composition – Mass fraction %.

Grade	C	Mn	Ni	Cu	P	S	Si	Fe
	Max	Max	Max	Max	Max	Max	Max	Bal.
L-80/1	0.43	1.9	025	0.35	0.03	0.03	0.45	
Alloy2	0.343	1.26	0.008	0.011	0.014	0.002	0.318	97.9

3.1.2 Mechanical properties

3.1.2.1 API 5L Standard 'Specification 5L covers steel line pipe' - Mechanical Properties

Table-3.3: Pipe body of seamless and welded pipes - Tensile Results

Grade	Yield Strength	Ultimate Tensile Strength	Elongation
	MPa	MPa	%
	Minimum	Minimum	Minimum
B	241	414	18
Alloy1	378.5	522.5	27

3.1.3 API 5CT Standard 'Specification 5CT for Casing and Tubing' - Mechanical Properties

Grade	Yield Strength		Ultimate Tensile Strength	Elongation
	MPa		Mpa	%
	Min	Max	Min	Min
L-80/1	552	655	655	17
Alloy2	649		703	20

3.1.4 Microstructure
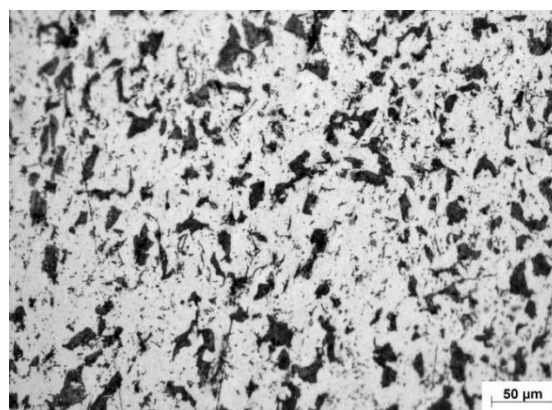
Fig. 3.1: Representative microstructure of Alloy1 containing both ferrite (bright areas) and pearlite (dark areas) phases.
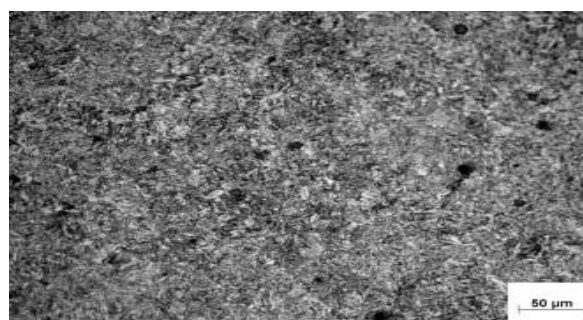
Fig. 3.2: Representative microstructure of Alloy2 showing finer grain size.

3.2 Electrolyte pH Evaluation

As shown in (Fig. 3.3 & Table 3.5), reduction in pH of saline solution on increasing NaCl concentration from 1.5 to 15 Wt. % was 0.4 (~ 8%), while in CO_2 – saturated solution it was 1.4 (~ 30 %) indicating a large, yet gradual increase in acidity of CO_2 – Saturated solution at high NaCl concentration of 10, 15 Wt. % NaCl.

This increase in acidity could be related to the presence of CO_3^{2-}, HCO_3^- and H^+ as a result of CO_2 reaction with H_2O.
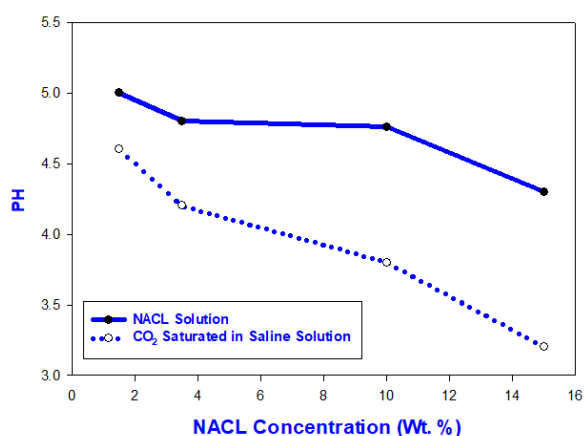
Fig. 3.3 pH of both saline / CO_2 saline solutions at ambient conditions.

Table 3.5: pH values of both saline / CO_2 saline solutions

Wt. % NaCl	pH before purging	pH after CO_2 saturation in Salinity Brines
1.5	5	4.6
3.5	4.8	4.2
10	4.76	3.8
15	4.3	3.2

3.3 Corrosion rates

Comparing corrosion rates of the investigated alloys in different NaCl concentrations (Fig. 3.4 & Table 3.6), identifying the standard deviation for corrosion rate test results [19], it can be noticed that both alloys showed a peak at 3.5 Wt. % NaCl, followed by a gradual reduction. Nevertheless, it is not lower than corrosion rates of both alloys at low concentrations (1.5 Wt.% NaCl). In addition, corrosion rates of both alloys examined at different concentrations was limited in a range of 0.033 to 0.156 mm/y. Corrosion in NaCl is related to the dissolved oxygen and the formation of the surface film on the substrate.
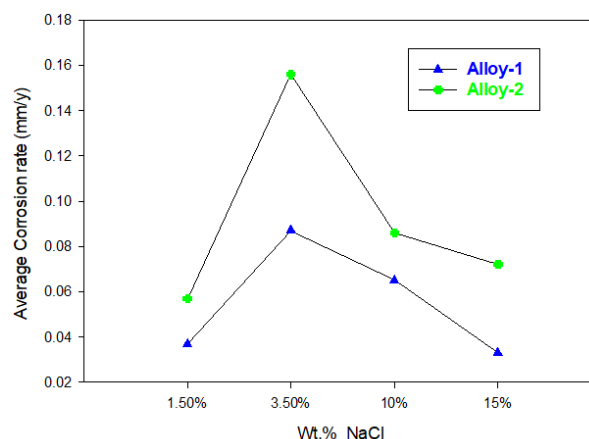
Fig. 3.4: Corrosion rates of the investigated alloys in saline solution.

Table 3.6: Corrosion rates of the investigated alloys in saline solution.

Test Runs	Corrosion rate in mm/year of Alloy1				Corrosion rate in mm/year of Alloy2			
Wt. % NaCl	1.5	3.5	10	15	1.5	3.5	10	15
Run-1	0.04	0.1	0.095	0.007	0.048	0.2	0.142	0.06
Run-2	0.035	0.1	0.08	0.04	0.051	0.1	0.09	0.056
Run-3	0.036	0.061	0.02	0.052	0.072	0.168	0.026	0.1
Average	0.037	0.087	0.065	0.033	0.057	0.156	0.086	0.072
STDEV	0.003	0.023	0.040	0.023	0.013	0.051	0.058	0.024

On the other hand, corrosion rates of both alloys in NaCl CO_2 – saturated solution (Fig.3.5 & Table 3.7) showed a much better performance of Alloy2 with a net reduction in corrosion rates at high NaCl concentrations (10, 15 Wt. %), limited within a range of 0.1 to 0.46 mm/y, whereas Alloy1 showed a wide corrosion range between 0.2 to 1.0 mm/y. it was relatively close to Alloy2 at high NaCl concentration (15 Wt. %) namely; 0.2 and 0.1 mm/y respectively.
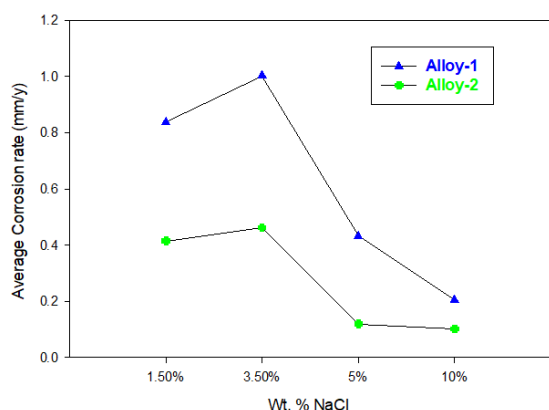
Fig. 3.5: Corrosion rates of the investigated alloys in CO_2 – saturated saline.

Table 3.7: Corrosion rates of the investigated alloys in CO_2 – saturated saline

Test Runs	Corrosion rate in mm/year of Alloy1				Corrosion rate in mm/year of Alloy2			
Wt. % NaCl	1.5	3.5	10	15	1.5	3.5	10	15
Run-1	1	1.1	0.486	0.165	0.5	0.486	0.089	0.19
Run-2	0.8	0.9	0.382	0.25	0.345	0.4	0.11	0.014
Run-3	0.717	1.009	0.428	0.2	0.4	0.5	0.161	0.102
Average	0.839	1.003	0.432	0.205	0.415	0.462	0.12	0.102
Standard Deviation	0.145	0.100	0.052	0.043	0.079	0.054	0.037	0.088

3.4 Potentiodynamic polarization

In this test, the electrode potential is changed over a relatively large domain, at a selected rate, by the application of a current through the electrolyte. It provides useful information regarding corrosion mechanism, corrosion rate and material susceptibility to corrosion in designated environments.

Test results of the investigated alloys in saline and CO_2 – saturated saline solutions at various NaCl concentrations are shown in Figs. 3.6 & 3.7 respectively.

It can be noticed that anodic and cathodic branches as well as Ecorr of the tested alloys have shown relative variations according to NaCl concentration. Corrosion parameters such as Ecorr, Icorr, Bc and Ba were estimated through Tafel plot and given in Tables 3.8 and 3.9 and illustrated in Fig. 3.8.
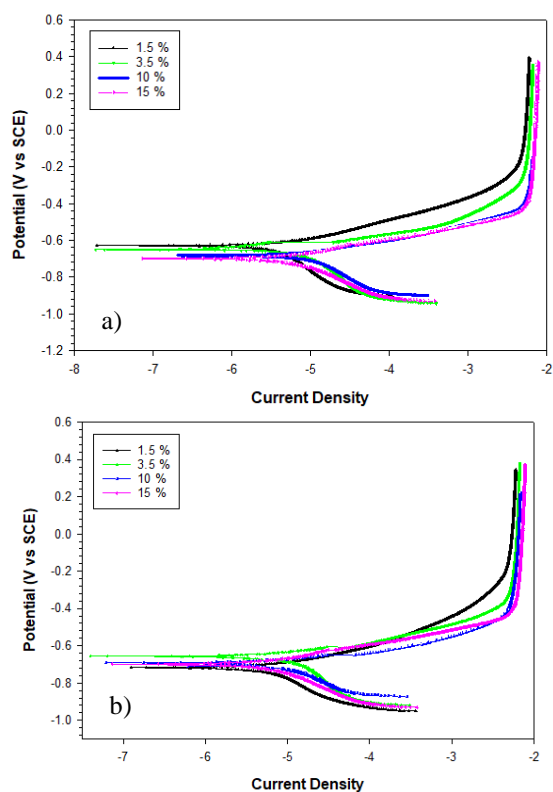
Fig. 3.6: Potentiodynamic polarization of the investigated alloys in saline (a) Alloy1, (b) Alloy2
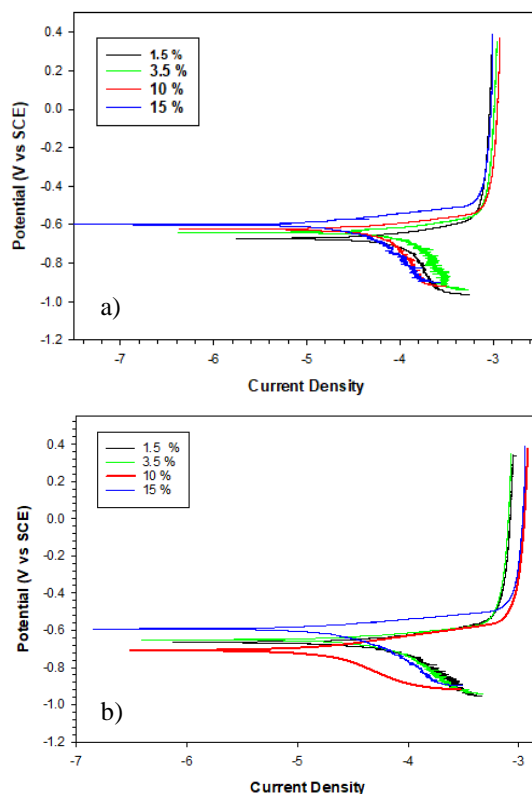
Fig. 3.7: Potentiodynamic polarization of the investigated alloys in CO_2 – saturated saline (a) Alloy1, (b) Alloy2.
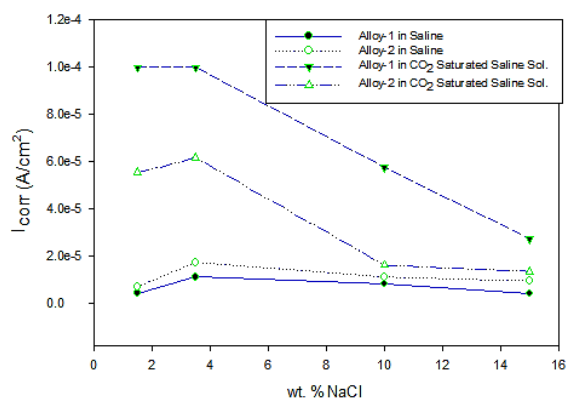
Fig. 3.8: i_{corr} of the investigated alloys in both saline and CO_2 – saturated saline

Table 3.8: Corrosion parameters the investigated alloys in saline solution

Wt. % NaCl	Alloy1				Alloy2			
	E_{corr} (V)	i_{corr} A/cm²	Bc V/dec	Ba V/dec	E_{corr} (V)	i_{corr} A/cm²	Bc V/dec	Ba V/dec
1.5	-0.63	4.39E^{-06}	0.299	0.079	-0.71	7.09E^{-06}	0.240	0.081
3.5	-0.65	1.12E^{-05}	0.361	0.075	-0.67	1.74E^{-05}	0.385	0.096
10	-0.68	8.31E^{-06}	0.161	0.068	-0.72	1.12E^{-05}	0.154	0.085
15	-0.69	4.24E^{-06}	0.119	0.058	-0.65	9.47E^{-06}	0.452	0.050

Table 3.9: Corrosion parameters of the investigated alloys in CO_2– saturated saline

Wt. % NaCl	Alloy1				Alloy2			
	E_{corr} (V)	i_{corr} A/cm²	Bc V/dec	Ba V/dec	E_{corr} (V)	i_{corr} A/cm²	Bc V/dec	Ba V/dec
1.5	-0.675	1.00E^{-04}	0.864	0.112	-0.755	2.46E^{-05}	0.325	0.119
3.5	-0.643	1.00E^{-04}	0.767	0.096	-0.662	9.68E^{-05}	0.532	0.077
10	-0.625	5.76E^{-05}	0.509	0.065	-0.612	5.39E^{-06}	0.238	0.053
15	-0.602	2.73E^{-05}	0.343	0.051	-0.062	5.67E^{-06}	0.234	0.06

It can be noticed that i_{corr} of both alloys in the saline solution at various NaCl concentration showed slight increase at 3.5 Wt. % NaCl. It is limited within 4.24-4.39 E^{-06} and 7.09 – 9.47 E^{-06} for Alloy1 and Alloy2 respectively. Meanwhile, in CO_2 – saturated saline solutions, both alloys showed a peak value at 3.5 Wt. % NaCl followed by a sharp drop down to 15 Wt. % NaCl. Nevertheless, Alloy2 has much lower i_{corr} at different concentrations of NaCl, attaining very close values to CO_2 – free saline solutions at 10 and 15 Wt. % NaCl.

E_{corr} variation as a function of NaCl concentrations in brine and CO_2 – saturated solution of the investigated alloys as given in Fig. 3.9 has shown an increase in E_{corr} of Alloy1(from -0.63 to -0.60 V), which is inversed to the more active direction (from -0.67 to -0.60 V) in CO_2 – NaCl solution. On the other hand, E_{corr} of Alloy2 has shown a sharp drop at 10 Wt. % NaCl in the absence and presence of CO_2 (~ -0.70 V), followed by a large

increase at 15 Wt. % NaCl where it has attained -0.59 V in the CO_2 - saturated solution. Variation in E_{corr} could be related to some defects in the surface film and /or imperfections taking place during the interfacial reactions.
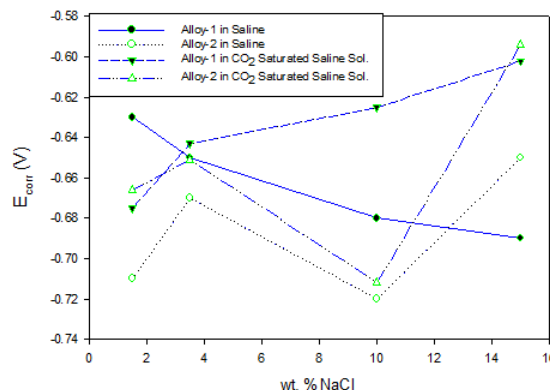
Fig. 3.9: Ecorr of the investigated alloys in both saline and CO_2 – saturated saline

3.5 Electrochemical Impedance Results

For a better understanding of interfacial reaction between the substrate and the electrolyte, Electrochemical Impedance Spectroscopy (EIS) test was carried out on the investigated alloys under the same conditions of electrolytes types and concentrations.

EIS results are represented by an equivalent electric circuit containing elements such as polarization resistance RP, solution resistance Rs, constant phase element (CPU), which models the behavior of a double layer. The results obtained through Nyquist plot (Fig. 3.10) and given in Table 3.10 were fitted by equivalent electric circuits given in Fig. 3.11 and Fig. 3.12, for the investigated alloys in saline solution, whereas results in CO_2 – saturated saline of both alloys are given in Fig. 3.13, Table 3.11 and Figs. 3.14 & 3.15 respectively.
It could be noted that increase in NaCl concentration results in a significant increase in solution conductivity, reflected as a reduction in Rs values. Also, addition of NaCl reduces the radius of the electrochemical impedance loops. Meanwhile, slight changes were observed in Nyquist plots when NaCl content exceeds 3.5 Wt. %, which could indicate that the metal surface susceptibility to corrosion has improved on further addition of NaCl (containing Cl⁻ ions). Also, Rp showed the lowest values at 3.5 Wt. % NaCl, followed by a slight increase on further increase of containing Cl⁻ ions.
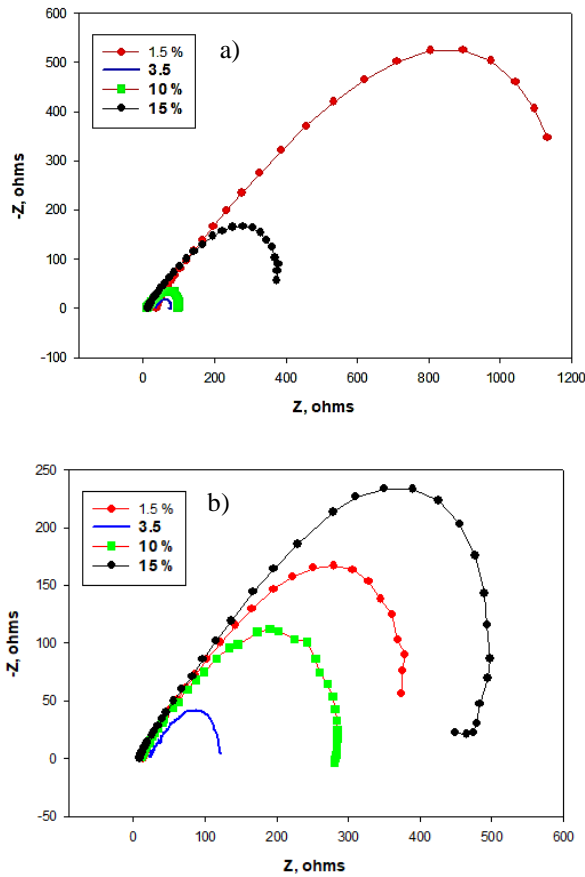
Fig. 3.10: Nyquist plot for both alloys in saline solution (a) Alloy1 , (b) Alloy2
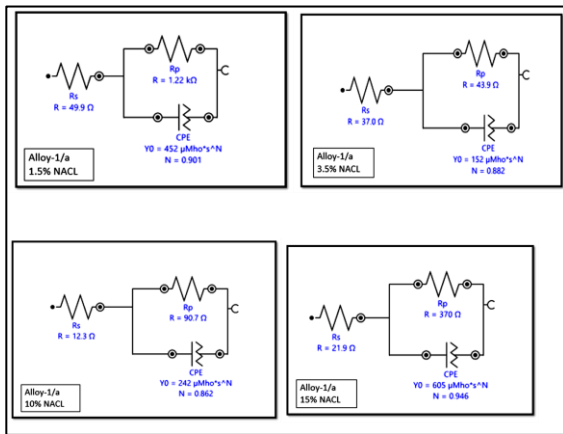
Fig. 3.11: Equivalent Circuits for Alloy1 in Saline Solutions
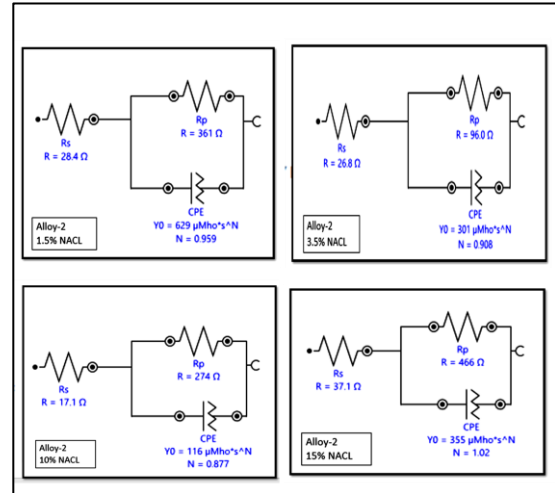
Fig. 3.12: Equivalent Circuits for Alloy2 in Saline Solutions.

Table 3.10: EIS parameters in saline solutions

Wt. % NaCl	Alloy1				Alloy2			
	Rp(Ω)	Rs(Ω)	CPE.Y0 (F)	CPE. N	Rp(Ω)	Rs(Ω)	CPE.Y0 (F)	CPE. N
1.5	1217.7	49.94	4.5E^{-04}	0.901	361.24	28.42	6.3E^{-04}	0.959
3.5	43.913	36.99	1.5E^{-04}	0.882	95.996	26.79	3E^{-04}	0.908
10	90.68	12.27	2.4E^{-04}	0.862	273.87	17.06	1.2E^{-04}	0.877
15	369.53	21.85	6.1E^{-04}	0.946	466.33	37.12	3.55E^{-04}	1.017
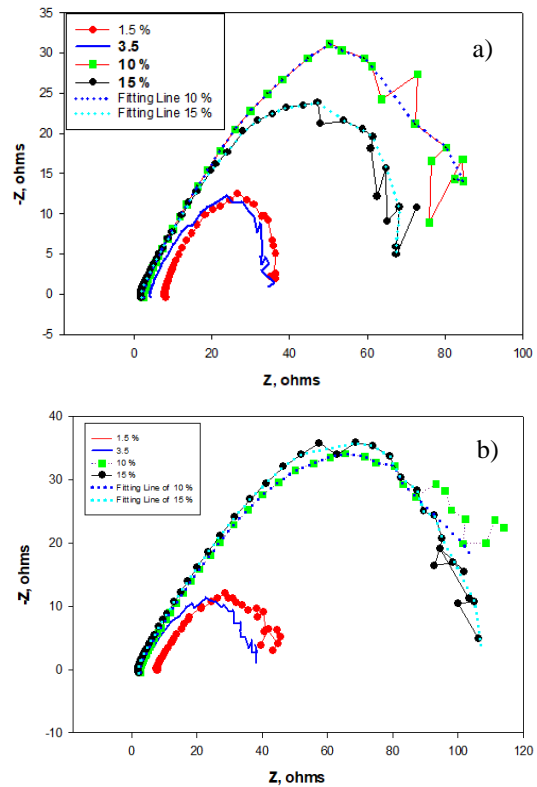
Fig. 3.13: Nyquist Impedance for Two Alloys in CO_2 – Saturated Saline Solutions, (a) Alloy1, (b) Alloy2.
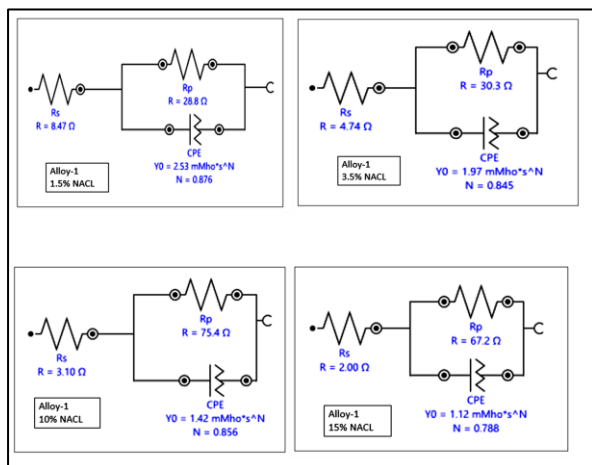
Fig. 3.14: Equivalent Circuits for Alloy1 in CO_2 – Saturated Saline Solutions
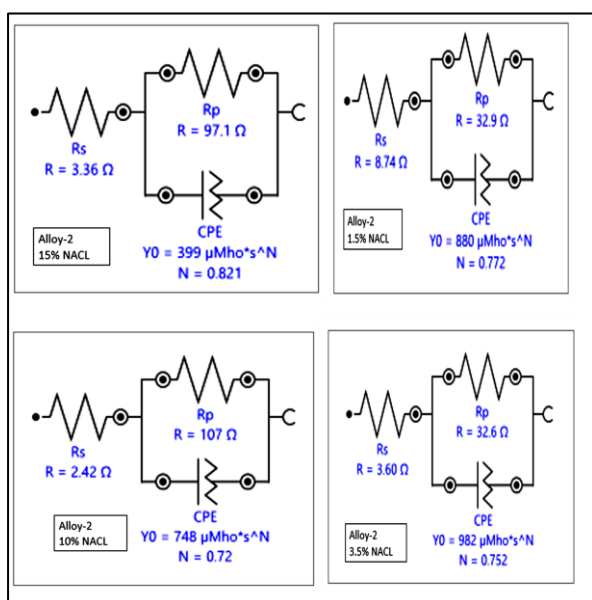
Fig. 3.15: Equivalent Circuits for Alloy2 in CO_2 – Saturated Saline Solutions

Table 3.11: EIS parameters in CO_2 - Saturated Saline Solutions

Wt. % NaCl	Alloy1				Alloy2			
	$Rp(\Omega)$	$Rs(\Omega)$	CPE.Y0 (F)	CPE. N	$Rp(\Omega)$	$Rs(\Omega)$	CPE.Y0 (F)	CPE. N
1.5	28.77	8.4	0.0025	0.876	32.88	8.7	0.0009	0.772
3.5	30.33	4.7	0.0019	0.845	32.57	3.6	0.0009	0.752
10	75.44	3.1	0.0014	0.856	107.49	2.4	0.0007	0.719
15	67.21	1.9	0.0011	0.787	97.11	3.4	0.0004	0.821

4. Discussion

Regarding evaluation of pH of both electrolytes as function of increase in NaCl concentration, saline solution showed a moderate reduction in pH attaining pH 4.3, while CO_2 – saturated solutions showed a very low pH value of 3.2 at 15 Wt. % NaCl which is far below 5.4 pH as an acceptable value, confirming the acidic effect of CO_2 as the chief corrosive agent in oil industry.

Comparing the corrosion rates of the investigated alloys in saline and CO_2 – saturated saline solutions, it is found that the corrosion rates of Alloy1 when tested in CO_2 – saturated saline solution has increased in in a range of ~ 22 to 6 folds with reference to its corrosion rates in saline solution, whereas Alloy2 showed a very limited increase of ~ 7 to 1.4 folds compared with its corrosion rates in saline, showing a much better performance in the CO_2 – aggressive environment.

Results of potentiodynamic polarization and Nyquist plots also confirmed a better performance of Alloy2 and a peak value of corrosion at 3.5 Wt. % NaCl in CO_2 – saturated solution, yet this peak was relatively insignificant in saline solution.

The better performance of Alloy2 as compared with Alloy1 is related to the difference in alloying additions, fine grain size microstructure and much better mechanical properties improving corrosion resistance of the alloys [20].

These observations related to reduction of corrosion rate CO_2 – saturated saline on increasing solution salinity could at least be partly attributed to the fact that NaCl decreases CO_2 solubility, lowering CO_2 content, which is known as salting out [21].

It is also reported that containing Cl^- ions significantly reduce CO_2 corrosion rate as a result of its retarding effect on the cathodic and anodic reactions at room temperature, due to the accumulation of (FeOH)ads on carbon steel surface resulting in a sharp increase in OCP (Fig. 3.9). Several studies have shown that CO_2 corrosion was more aggressive in water than in brine [22] and that iron alloys present high corrosion rates in presence of solutions containing CO_2 than in presence of acid solutions at the same pH [23-24].

This has led many authors to study the cathodic and anodic processes separately to better understand the mechanism of iron alloys corrosion in presence of CO_2 containing solutions.

Concerning the cathodic process, two mechanisms were widely adopted: the direct reduction mechanism, based on an additional reaction involving CO_2 [25-26] and the buffering effect mechanism in which the dissociation of carbonic acid acts as an extra source of H ions. [27-28]. Recent published results have shown that cathodic mechanism is better explained by the buffering effect induced by dissolved CO_2 [29-30].

Anodic process studies involved iron dissolution in acid media, in absence of CO_2 dissolved gas [11,18]. Few papers have partially dealt with this concern. [31-32]. Regarding the role of containing Cl^- ions in CO_2 corrosion of carbon steel, previous literature [33-34] have reported that containing Cl^- ions formed intermediate corrosion species with metal ions, enhancing the transfer of metal ions into solution and accelerating anodic reaction rates. Meanwhile sites occupied by Cl^- ions are turned more anodic, accelerating dissolution of metal substrate.

Dissolved Fe^{2+} would diffuse through the electrolyte and then be adsorbed to the cathodic sites on the steel surface [35-36], which results in less active sites to be available for reduction of carbonic acid and bicarbonate ions between substrate and solution, leading to a stable value of corrosion rate in spite of further addition of containing Cl^- ions.

5. Conclusions

Carbon dioxide corrosion is the most aggressive corrosion type affecting oil and gas industry, in this study two types of carbon steel alloys used in the production and transportation of oil namely; API5L Grade-B (referred to as Alloy1) and API 5 CT Grade L-80/1 (referred to as Alloy2) were investigated to evaluate their corrosion behaviour in Cl^- ions – containing CO_2 – saturated solutions at ambient temperature and pressure.

The study employed electrochemical measurements including potentiodynamic polarization technique and electrochemical impedance spectroscopy (EIS) using NaCl electrolyte at 1.5, 3, 10, & 15 Wt. %.

The results obtained in this investigation could be summarized as follows.

- On increasing NaCl concentration from 1.5 to 15 Wt. %, pH of brine attained 4.3, whereas in CO_2 – saturated solution it was 3.2, indicating a reduction of 8 and 30 % respectively. This large drop in pH is related to the species resulting from CO_2 reaction with water.

- Corrosion rates of both alloys in brine solution showed a relative increase at 3.5 Wt. % NaCl, meanwhile their values at lower and higher Wt. % NaCl were almost similar. Alloy1 showed relative better performance than Alloy2. Corrosion rates of both alloys were limited in a range of 0.033 to 0.156 mm/y. This behaviour in saline solution is related to the dissolved O2 and surface film formation.

- Corrosion of the investigated alloys in CO_2 – saturated brine showed a much better performance of Alloy2 with a net reduction in corrosion rates at high NaCl concentrations limited with a range of 0.1 to 0.46 mm/y, whereas Alloy1 showed a wide variation in corrosion rates between 0.2 to 1.0 mm/y it was relatively close to Alloy2 at 15 Wt. % NaCl. The better performance of Alloy2 is related to the difference in of alloying additions, fine grain size and much better mechanical properties.

- The stable values of corrosion rates obtained in spite of increasing Cl^- ions concentration could be partly related to reduction of CO_2 solubility or salting out and the role of Cl^- ions in accelerating Fe^{+2} dissolution which would be adsorbed to the cathodic sites on the steel surface reducing active sites on the substrate available for reduction of carbonic acid and bicarbonate.

References

[1] Bi, C. H. E. N., Bijuan, Z. H. E. N. G., Fan, Z. H. A. N. G., & Hongfang, L. I. U., Corrosion Behavior of HSn70-1 Copper Alloy in SRB Containing Medi (2014), Mao, X., Liu, X., & Revie, R. W., Pitting corrosion of pipeline steel in dilute bicarbonate solution with chloride ions. Corrosion, 50(09). um in Atatic Magnetic Field. Journal of Chinese Society for Corrosion and protection, 34(4), (1994) 339-345.

[2] Wei, L., Gao, K., & Li, Q., Corrosion of low alloy steel containing 0.5% chromium in supercritical CO_2-saturated brine and water-saturated supercritical CO_2 environments. Applied Surface Science, 440, (2018) 524-534.

[3] Mao, X., Liu, X., & Revie, R. W., Pitting corrosion of pipeline steel in dilute bicarbonate solution with chloride ions. Corrosion, 50(09) (1994) 651-655.

[4] Hu, Y. B., Dong, C. F., Sun, M., Xiao, K., Zhong, P., & Li, X. G., Effects of solution pH and Cl^- on electrochemical behaviour of an Aermet100 ultra-high strength steel in acidic environments. Corrosion science, 53(12), (2011) 4159-4165.

[5] R. H. Hausler, Advances in CO_2 Corrosion,. Vol. 1, NACE, Houston, Texas 1984, pp. 72.

[6] - Bian, C., Wang, Z. M., Han, X., Chen, C., & Zhang, J., Electrochemical response of mild steel in ferrous ion enriched and CO2 – saturated solutions. Corrosion Science, 96, (2015) 42-51.

[7] Liu, Q. Y., Mao, L. J., & Zhou, S. W., Effects of chloride content on CO2 corrosion of carbon steel in simulated oil and gas well environments. Corrosion science, 84, (2014) 165-171.

[8] Eliyan, F. F., Mohammadi, F., & Alfantazi, A., An electrochemical investigation on the effect of the chloride content on CO2 corrosion of API-X100 steel. Corrosion Science, 64, (2012) 37-43.

[9] Mao, X., Liu, X., & Revie, R. W., Pitting corrosion of pipeline steel in dilute bicarbonate solution with chloride ions. Corrosion, 50(09) (1994) 656-657.

[10] Zhang, N., Zeng, D., Zhang, Z., Zhao, W., & Yao, G., Effect of flow velocity on pipeline steel corrosion behaviour in H_2S/CO_2 environment with sulphur deposition. Corrosion Engineering, Science and Technology, 53(5), (2018) 370-377.

[11] Chen, C. F., Lu, M. X., Sun, D. B., Zhang, Z. H., & Chang, W., Effect of chromium on the pitting resistance of oil tube steel in a carbon dioxide corrosion system. Corrosion, 61(06) (2005) 594-601.

[12] Chen, C. F., Lu, M. X., Zhao, G. X., Bai, Z. H. E. N. Q. U. A. N., Yan, M. I. L. I. N., & Yang, Y. A. N. Q. I. N. G., Characters of CO_2 Corrosion Scales on Well Tube Steels N80. ACTA METALLURGICA SINICA-CHINESE EDITION-, 38(4), (2002) 411-416.

[13] - Ma, H. Y., Yang, C., Li, G. Y., Guo, W. J., Chen, S. H., & Luo, J. L., Influence of nitrate and chloride ions on the corrosion of iron. Corrosion, 59(12) (2003). '

[14] Farelas, F., Galicia, M., Brown, B., Nesic, S., & Castaneda, H., Evolution of dissolution processes at the interface of carbon steel corroding in a CO_2 environment studied by EIS. Corrosion Science, 52(2), (2010) 509-517.

[15] Liu, Q. Y., Mao, L. J., & Zhou, S. W., Effects of chloride content on CO2 corrosion of carbon steel in simulated oil and gas well environments. Corrosion science, 84, (2014) 165-171.

[16] Ingham, B., Ko, M., Laycock, N., Burnell, J., Kappen, P., Kimpton, J. A., & Williams, D. E., In situ synchrotron X-ray diffraction study of scale formation during CO_2 corrosion of carbon steel in sodium and magnesium chloride solutions. Corrosion Science, 56, (2012) 96-104.

[17] SCHMITT, G., Untersuchungen zum korrosionsmechanismus von unlegiertem stahl in sauerstoffreien kohlensaeureloesungen. I. Kinetik der wasserstoffabscheidung(1977).

[18] Schmitt, G., Investigations Into the Corrosion Mechanism of Mild Steel in Oxygen Free Carbon Dioxide Solutions. II. Kinetics of Iron Dissolution. Werkst. Korros., 29(2), (1978) 98-100.

[19] Wong, L. L., Martin, S. I., & Rebak, R. L. B. (, January). Methods to calculate corrosion rates for alloy 22 from polarization resistance experiments. In ASME Pressure Vessels and Piping Conference, 47586, (2006) 571-580.

[20] Soleimani, M., Mirzadeh, H., & Dehghanian, C., Effect of grain size on the corrosion resistance of low carbon steel. Materials Research Express, 7(1), (2020) 016522.

[21] Sun, Q., Tian, H., Li, Z., Guo, X., Liu, A., & Yang, L., Solubility of CO_2 in water and NaCl solution in equilibrium with hydrate. Part I: Experimental measurement. Fluid Phase Equilibria, 409, (2016) 131-135.

[22] das Chagas Almeida, T., Bandeira, M. C. E., Moreira, R. M., & Mattos, O. R., New insights on the role of CO_2 in the mechanism of carbon steel corrosion. Corrosion Science, 120, (2017) 239-250.

[23] De Waard, C., & Milliams, D. E., Carbonic acid corrosion of steel. Corrosion, 31(5), (1975) 177-181.

[24] Linter, B. R., & Burstein, G. T., Reactions of pipeline steels in carbon dioxide solutions. Corrosion science, 41(1), (1999) 117-139.

[25] Zhang, Y., Gao, K., & Schmitt, G., Water effect on steel under supercritical CO_2 condition. In CORROSION 2011. OnePetro.

[26] Nesic, S., Postlethwaite, J., & Olsen, S., An electrochemical model for prediction of corrosion of mild steel in aqueous carbon dioxide solutions. Corrosion, 52(4), (1996) 280-294.

[27] Tran, T., Brown, B., & Nesic, S., Corrosion of mild steel in an aqueous CO_2 environment–basic electrochemical mechanisms revisited. In CORROSION 2015. OnePetro.

[28] Linter, B. R., & Burstein, G. T., Reactions of pipeline steels in carbon dioxide solutions. Corrosion science, 41(1), (1999) 117-120.

[29] Linter, B. R., & Burstein, G. T., Reactions of pipeline steels in carbon dioxide solutions. Corrosion science, 41(1), (1999) 131-139.

[30] Remita, E., Tribollet, B., Sutter, E., Vivier, V., Ropital, F., & Kittel, JHydrogen evolution in aqueous solutions containing dissolved CO2: Quantitative contribution of the buffering effect. Corrosion science, 50(5), . (2008) 1433-1440.

[31] Gray, L. G., Anderson, B. G., Danysh, M. J., & Tremaine, P. R., Mechanisms of carbon steel corrosion in brines containing dissolved carbon dioxide at pH 4. CORROSION/89, paper, (464), (1989) 1-18.

[32] Nesic, S., Thevenot, N., Crolet, J. L., & Drazic, D., Electrochemical properties of iron dissolution in the presence of CO_2-basics revisited. In CORROSION 96, (1996) OnePetro.

[33] Ashley, G. W., & Burstein, G. T., Initial stages of the anodic oxidation of iron in chloride solutions. Corrosion, 47(12), (1991) 908-916.p

[34] Hou, L., Raveggi, M., Chen, X. B., Xu, W., Laws, K. J., Wei, Y., ... & Birbilis, N., Investigating the passivity and dissolution of a corrosion resistant Mg-33at.% Li alloy in aqueous chloride using online ICP-MS. Journal of the Electrochemical Society, 163(6), (2016) C324.

[35] Bian, C., Wang, Z. M., Han, X., Chen, C., & Zhang, J., Electrochemical response of mild steel in ferrous ion enriched and CO2 – saturated solutions. Corrosion Science, 96, (2015). 42-51.

[36] Gao, M., X. Pang, and K. Gao. "The growth mechanism of CO2 corrosion product films." Corrosion Science 53(2), (2011) 557-568.